Supporting Information: On the Growth Regimes of Hydrogen Bubbles at Microelectrodes

Aleksandr Bashkatov*[1,2,3], Syed Sahil Hossain[1], Gerd Mutschke[1], Xuegeng Yang[1], Hannes Rox[1], Inez M. Weidinger[4] and Kerstin Eckert†[1,2,3]

[1]Institute of Fluid Dynamics, Helmholtz-Zentrum Dresden-Rossendorf, Bautzner Landstrasse 400, Dresden, 01328 Germany
[2]Institute of Process Engineering and Environmental Technology, Technische Universität Dresden, Dresden, 01062 Germany
[3]Hydrogen Lab, School of Engineering, Technische Universität Dresden, Dresden, 01062 Germany
[4]Fakultät Chemie und Lebensmittelchemie, Technische Universität Dresden, Zellescher Weg 19, 01069 Dresden, Germany

*a.bashkatov@hzdr.de
†k.eckert@hzdr.de

1. Simulation methodology

We provide here a brief overview of the simulations carried out to calculate the hydrodynamic and electric forces presented in the main text. The method is described in detail in our previous studies[1–3]. Laplace equation of the electric potential, Navier-Stokes equation along with continuity and the heat equations are solved simultaneously in FEM-based solver COMSOL 5.5. The surface tension of the bubble-electrolyte interface is a linear function of the temperature. Since the current density distribution is strongly non-uniform along the electrode surface and the bubble interface, concentrated Joule heating causes temperature gradient along the interface, which in turn gives rise the surface tension gradient. This surface tension gradient causes electrolyte to flow also otherwise known as Marangoni flow. This flow is responsible for the hydrodynamic force felt by the bubble. The electric force originates from the action of the electric field in the electrolyte, in the vicinity of the bubble interface, on the adsorbed protons at the bubble interface.

The resulting dependence of F_e and F_h on δ is shown in Figure 2. The data are obtained by carrying out parametric simulations of $F_e(\delta)$ and $F_h(\delta)$ for varying δ in COMSOL 5.5. Further simulation parameters are given in the caption. The simulation methodology is similar to Hossain et al.[3] except that ε is not implemented since the deformation also varies with δ with unknown dependence This means that the bubble is a perfect sphere that resides on the carpet. The vertical position of the bubble center is $\delta + \sqrt{R^2 - \Theta R_e^2}$, where R_e is the radius of the microelectrode, and Θ is the gas coverage of the cathode (see Hossain et al.[3]). This way the bubble exactly covers the top surface of the carpet in the model.

2. Frequency and the amplitude of the electric current oscillations

We next examine the frequency and the amplitude of the electric current oscillations. Both are documented in Figure S1 exemplarily for various potentials at a concentration of 0.5 mol L^{-1}. The frequency is calculated from $f = 1/\Delta t$, with Δt denoting the time interval between two consecutive maxima (or minima). The amplitude is calculated as the difference of the electric current between maximum and minimum. To enable a unified presentation for the different times of onset t_{onset} and duration T_{osc} of the oscillations, the dimensionless time $(t-t_{onset})/T_{osc}$ is introduced, where 0 and 1 uniquely mark the onset of the oscillations and the bubble departure. All data shown are obtained from averaging over 8 bubbles. In line with the findings of Figure 3c(1) and 3c(2), the amplitude of the current significantly increases during the oscillations. Indeed the current may take values which are 14 times larger than the values found in the plateau region of Regime I. The frequency of the bubble oscillations reduces over time for all the potentials applied. This may be vividly explained by the bubble growth with time.

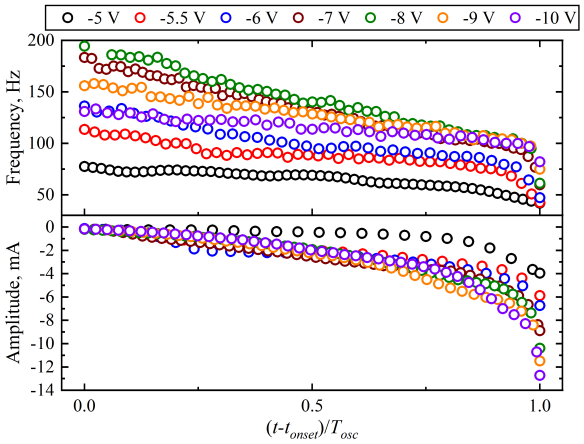

Figure S1: Frequency and amplitude of the electric current over the dimensionless time $(t - t_{onset})/T_{osc}$ for various potentials in 0.5 mol L^{-1} in Regime II. The data shown are obtained from averaging over 8 bubbles. The potential is vs. pseudo RE (Pt wire).

3. Bubble response to jumps in potential

To learn more on the transient bubble behavior, sudden jumps of the potential were imposed in regimes I-III, and the system's response was studied. In addition to the first set of experiments on the carpet response discussed in Section 4.5 of the manuscript and shown in Fig. 12, two other sets are presented here.

The second set of experiments performed is devoted to the current response in Regime II, see Fig. S2a. Hydrogen bubbles generated at $\Delta\phi_1$ = -4 V and 1 mol L^{-1} in Regime II served as reference case. As shown in the top plot of Fig. S2 the current oscillates with increasing amplitude until the bubble detaches at about 3.78 s. We now probe the system shortly before detachment (3.7 s) by a jump from $\Delta\phi_1$ to $\Delta\phi_2 = -5$ V and $\Delta\phi_3 = -6$ V, respectively.

Immediately after the jump, the previous oscillations are suppressed either partially (-5 V) or completely (-6 V). This is in line with Fig. 3a in which the oscillations at -5 V are more intense than at -6 V. These experiments support the fact that the oscillations are a systematic and robust phenomenon. They occur in a reproducible manner in the parameter ranges belonging to Regime II.

The third set of experiments is devoted to the transition between Regime III and II. Bubble growth is conducted first in Regime III at $\Delta\phi_1 = -10$ V, see the red curve in Figure S2b. A jump in the potential toward $\Delta\phi_2 = -6$ V is applied at a bubble diameter of about 450 μm as marked by the dashed line. At this diameter, the bubble would be in the fully oscillatory mode of Regime II when having grown it at potential of -6 V from the very beginning, see black line in Figure S2b. Thus the figure proves the transitions from Regime III to Regime II simply by the suddenly lowering the potential. At the moment the potential is swapped from $\Delta\phi_1 = -10$ V to $\Delta\phi_2 = -6$ V, the current peaks for a short moment, see the red curve. Afterwards the current relaxes quickly to the value of the reference case (black curve), at the corresponding bubble radius. The red $R(t)$ curve displays an increase in the slope, hence growth rate, similar to the reference case. This demonstrates that a bubble grown at high potential $\Delta\phi_1 = -10$ V needs more time than at $\Delta\phi_2 = -6$ V to reach the same diameter.

4. Forces calculation

For the bubble growing on a solid surface, the downward-directed surface tension force and the upward-directed contact pressure and buoyancy forces have been estimated to support a discussion part in the body of the manuscript. The calculations performed for the growing

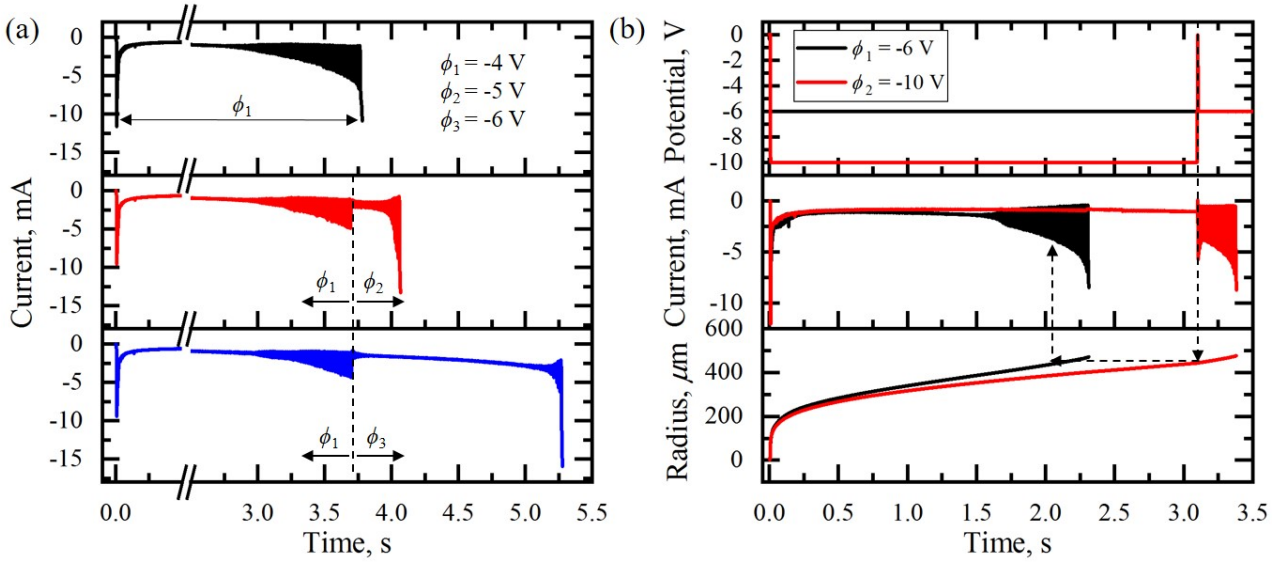

Figure S2: (a) Response to jumps in the potential in the oscillatory phase of Regime II (1 mol L^{-1}). Top image shows growth at $\Delta\phi_1$ (reference case). Red and blue curves show the response to $\Delta\phi_1 = -4$ V $\rightarrow \Delta\phi_2$ after 3.7 s. $\Delta\phi_2 = -5$ V (red) and $\Delta\phi_3 = -6$ V (blue curve). Due to different electrodes, T and t_{onset} differ slightly from Fig. 3a but underly the robustness of the oscillations. (b) Response to jumps in the potential between regimes III and II: Cathodic potential, electric current and radius over time for the reference bubble produced at -6 V and for another bubble produced at -10 V and alternated to -6 V after 3.1 s polarization time. Experiments are done in 0.5 mol L^{-1}. The potential is vs. pseudo RE (Pt wire).

bubble, at the instant of time $t = 5$ s from Fig. 3d and Fig. 9a with the bubble radius at that instant of time $R = 537\ \mu$m, contact angle $\theta = 15°$, contact radius $r_c = 49\ \mu$m, gas-electrolyte density difference $\Delta\rho = 10^3$ kg m^{-3} and surface tension $\gamma = 72$ mN m^{-1}.

Substituting the values into the equations 1, 4 and 5 from the manuscript (also reproduced here as equations 7, 3 and 4), the buoyancy force, the surface tension force and contact pressure force were estimated to be $F_b = 6.36\ \mu$N, $F_s = -5.74\ \mu$N and $F_{cp} = 2.02\ \mu$N.

References

[1] J. Massing, G. Mutschke, D. Baczyzmalski, S. S. Hossain, X. Yang, K. Eckert and C. Cierpka, *Electrochimica Acta*, 2019, **297**, 929–940.

[2] S. S. Hossain, G. Mutschke, A. Bashkatov and K. Eckert, *Electrochimica Acta*, 2020, **353**, 136461.

[3] S. S. Hossain, A. Bashkatov, X. Yang, G. Mutschke and K. Eckert, *Physical Review E*, 2022.